

Patching Asymptotics Solution of a Cable with a Small Bending Stiffness

*Vincent Denoël** Member, ASCE

and Thomas Canor[†]

Abstract

The analysis of a cable with a small bending stiffness is a problem encountered in many engineering applications such as the fatigue assessment of stay cables, the modeling of pipeline laying operation or the determination of bending stresses in drillpipe assemblies. Because this phenomenon is modeled by a singularly perturbed equation, standard numerical techniques fail to solve these problems efficiently. As an alternative, provided the complexity of the analytical developments does not preclude their application, these problems may be tackled with appealing analytical procedures such as matching asymptotics or multiple scales. Otherwise advanced numerical simulations combining patching asymptotics within a numerical framework are the only possible approach for problems where the governing equations are too complex. Patching asymptotics also features a number of merits such as the possibility of using a boundary layer with a finite extent. Aiming at a better understanding of this latter technique, it is considered here to determine the solution of a cable with a small bending stiffness. Interesting details about patchability conditions and about how to restore higher derivatives continuity are included. The accuracy of the patching asymptotics approach is also compared with that of matched asymptotics.

Keywords: multiple scales; matching; patching; asymptotics; boundary layer; beam-cable;

*Department of Architecture, Geology, Environment and Constructions, Structural Engineering Division, University of Liege, Belgium. E-mail: v.denoel@ulg.ac.be.

[†]F.R.S.-FNRS National Fund for Scientific Research and Department of Architecture, Geology, Environment and Constructions, Structural Engineering Division, University of Liege, Belgium. E-mail: t.canor@ulg.ac.be.

small bending stiffness; heavy elastica; rod; nonlinear boundary value problem; patchability.

Introduction

Perturbation methods have been widely used and documented over the last decades (Hinch 1991; Kevorkian and Cole 1996; Nayfeh 1973). In this paper we compare the application of some methods to solve a problem with boundary layers. Such a problem is traditionally tackled by means of the method of matched asymptotics, (Esipova 1975; Schmeiser and Weiss 1986), which consists in finding asymptotic solutions along the different parts of the domain, matching them and, if possible, providing a composite approximation that is valid throughout the whole domain. As a matter of fact, this way of considering different scales on different parts of the domain is just a particular case of a more general approach, the multiple scales method. This latter approach considers a continuous blend of various scales throughout the whole domain and is *ipso facto* devoted to a wider class of problems than only those involving boundary layers. The multiple scales approach is evidently found to be superior, as compared to the matching asymptotics, but requires more tedious mathematical developments. In particular, the cancellation of secular terms pertaining to the multiple scales approach is not a simple task in case of complex governing equations, compelling then one to fall back on matching asymptotics as soon as analytical developments are too complex.

Another option consists in patching solutions obtained in different parts of the domain (Quararone and Valli 1994). The development of a patching solution starts by recognizing the existence of (at least) two domains, usually referred to as the *inner* and *outer* domains. Distinct governing equations are written for each sub-domain, providing thus inner and outer solutions that are valid on strictly non-overlapping subsets of the domain. A distinctive property of this approach is therefore to provide a boundary layer with a finite extent, which makes it an ideal tool for numerical simulation. Also, for many pragmatical reasons, it is sometimes essential to handle a boundary layer with a finite extent.

Moreover it is appealing to model the physical phenomena in the different sub-domains with the appropriate asymptotic governing equations. All the more, and because the patching asymptotic

method is the perfect framework for a numerical solution of the problem –in view of its finite extent boundary layer–, the asymptotic governing equations are eventually recast into a well conditioned format, by means of stretched co-ordinates. They are then considered as a set of regular boundary values problems, see e.g. Kumar et al. 2009; Reddy and Chakravarthy 2004. The patching asymptotics method is the perfect layout to show imagination. Indeed governing equations for the inner and outer solutions can in principle be made as various and simple as desired. However, despite the lack of accuracy that would result from too approximate models, the lack of patchability of the solutions over the different sub-domains is also possible. This issue is discussed and illustrated next, as a main contribution of this paper.

In this paper, we consider a particular problem, as probably not so many could be thought of, where the three above mentioned perturbation methods may be applied. It consists in the structural analysis of a cable with a small bending stiffness, which is also sometimes referred to as a *rod* or *elastica*. This problem is encountered in many engineering applications, in particular the modeling of bending stresses in anchorage zones of stay-cables. These stresses are typically critical for the fatigue aging of stay-cables (Cluni et al. 2007; Traeger and Kollegger 2010; Wei and Qiang 2011). Other applications encompass the bending of power line conductors (Hong et al. 2005; Papailiou 1997), pipelines or stents, Wang et al. 2011. In these applications, bending stresses take place along very short zones, compared to the total length, which makes the use of standard finite difference or finite element techniques rather inefficient, as pointed out clearly in Burgess 1993. Some advanced numerical techniques have been developed to cope with these large gradients (Bieniassz 2008; Jain et al. 1984; Rao and Kumar 2007; Stynes and Oriordan 1986), but their application is still troublesome as the boundary layer becomes very short.

The existence of short high-gradient zones in cables has already been observed and solved by means of matching asymptotics (Rienstra 1987; Wolfe 1991). Alternatively, application of a multiple scales approach has recently proven to be applicable too, and even to provide more accurate results up to moderate values of the small dimensionless bending stiffness (Denoël and Detournay 2010). Essentially this paper establishes the solution of the problem with another

perturbation technique, the patching asymptotics method. The developments are performed with a specific focus on the advantages and drawbacks of this method. Furthermore, they are carried out explicitly, although in a practical context that method would be applied numerically (Kumar et al. 2009). However, in doing so, the patchability conditions are studied analytically, independently thus of the quality of the numerical simulation.

In contrast to former works, we consider in this paper the special case where the cable length is not *a priori* given. Instead, the vertical and horizontal offsets between the anchorages are supposed to be given. This problem corresponds much better to real-life applications, for instance a stay-cable that has to be tensioned between its supports in order to bridge the known distance between the deck and the pylon. As shown next, this particular feature of the considered problem will make the use of the patching asymptotic method quite efficient, as compared to other asymptotic methods.

The Considered Problem

Transverse loads applied on cables are usually supposed to be internally balanced by axial forces only, in a largely displaced and deformed configuration. Figure 1-a depicts a typical engineering problem, where the deformation of an inextensible cable of (unknown) length ℓ , sagging between supports separated by a known distance L , has to be determined, under a given tension force H . In the case of a horizontal chord, the vertical reaction V is equal to half of the total weight, $V = w\ell/2$, by symmetry. The solution is obtained by writing that the internal shear force F_2 in the cable is equal to zero

$$F_2 = (V - ws) \cos \theta + H \sin \theta = 0 \quad (1)$$

where w is the weight of the cable per unit length, $\theta(s)$ is the inclination with respect to the horizontal and $s \in [0; \ell]$ is a curvilinear abscissa measured along the deformed cable. The deformed configuration is readily obtained as the solution $\theta(s)$ of (1). Internal axial forces are then obtained by similar equilibrium equations. In the considered problem, the cable length ℓ is *a priori* unknown; it has to be determined in such a way that the inclination of the cable $\theta(s)$ complies with the

Fig. 1: (a) the catenary problem where the deflection of a cable under tension H is to be determined and (b) the considered problem which is similar but with imposed end rotations. Notice the cable length ℓ is unknown in both cases.

given horizontal offset, by solving

$$\int_0^\ell \cos \theta ds = L \quad (2)$$

for ℓ .

This way of modeling cables, commonly referred to as the catenary solution, holds as long as the cable ends are free to rotate. Indeed, as soon as the end reactions V and H are given, this model excludes the possibility of imposing the inclination of the cable at any point. In other words, this model cannot be used to analyze a cable with imposed anchor rotations, as sketched in Fig. 1-b, or even in-span concentrated loads, which are common in everyday engineering applications. The catenary model necessarily needs to be enriched in order to examine end conditions related to higher order derivatives such as rotations or shear forces. To this purpose, the bending stiffness of the cable, although usually very small, is formally introduced and the internal shear force of the cable is related to the curvature, exactly as for a large displacement Euler-Bernoulli beam (Timoshenko and Goodier 1987)

$$F_2 \equiv EI\theta'' = (V - ws) \cos \theta + H \sin \theta. \quad (3)$$

This more sophisticated model, also known as the heavy elastica (Levien 2008; Wang 1986), offers two boundary conditions and therefore the possibility of fixing both end inclinations θ_0 and θ_ℓ . This nonlinear equation has analytical solutions in only few particular cases. The analysis of an elastica is therefore usually performed with numerical methods. These numerical methods fail to be efficient in solving this kind of problem when the dimensionless bending stiffness $EI/w\ell^3$ is small. In this case very short boundary layers take place in the neighborhood of cable ends and concentrated loads. This is a consequence of the relative smallness of the coefficient of θ'' , which makes this equation a singularly perturbed equation (Kevorkian and Cole 1996). The gradients

of internal forces –especially the bending moment– are so large in these boundary layers that it prevents the rational application of standard numerical methods.

There is an additional difficulty in the problem at hand, because (3) has to be solved for $s \in [0; \ell]$, where ℓ is determined by condition (2).

In fact, there are three characteristic forces in the governing equation (3), namely EI/ℓ^2 , $w\ell$ and H . When considering $w\ell$ as the scaling force, there exists therefore two dimensionless numbers

$$\varepsilon^2 = \frac{EI}{w\ell^3} \quad \text{and} \quad \eta^2 = \frac{H}{w\ell} \quad (4)$$

related to the bending rigidity of the cable and the horizontal tension force (only positive tension forces are considered in this paper). Depending on the smallness of these two parameters, the governing equation (3) degenerates into some well-known limit cases (Rienstra 1987). First, the catenary equation (1) appears as an evident particular case of (3) for $EI = 0$. Second, if the inclination $\theta(s)$ varies slightly around $\tilde{\theta}_0$ on $[0; \ell]$, as a result of a large bending stiffness ε or tension force η , (3) may be linearized around $\tilde{\theta}_0$. From there, two complementary assumptions corresponding either to vanishing bending stiffness or tension force respectively yield the classical shallow cable and nonlinear beam equations (Antman 1995). Third, the governing equation of the weightless classical elastica, which is known to be similar to the nonlinear pendulum equation is obtained by setting $w = 0$ in (3). All these particular cases of (3) possess analytical solutions respectively expressed by means of trigonometric, polynomial, hyperbolic, exponential or elliptic functions.

The matching asymptotic and multiple scales methods consists in observing that these particular cases are recovered by scaling properly the length scales in the problem. The solutions obtained for the different scales are expressed throughout the whole domain, then somehow combined in order to provide a composite solution. On the contrary, in a patching asymptotic approach, the particular cases mentioned above are assumed to take place along finite portions of the domain, then reconnected in order to restore the continuity up to a certain order.

For the sake of keeping developments simple, we restrict ourselves to the consideration of a cable with supports at the same level, which entails $V/w\ell = 1/2$, and with horizontal end inclinations

Fig. 2: (a) Decomposition of the beam into several sub-domains that are patched; (b) catenary solution in the outer domain; (c) beam solution in the inner domain.

($\theta_0 = \theta_\ell = 0$), see Fig. 1-b. This is sufficient to make the main argument of the paper come clear.

Patching Asymptotics Solution

Engineering solutions of the catenary problem (Irvine 1975) as well as the usual beam theories (Timoshenko and Goodier 1987) express the deflection of the considered member with respect to a straight reference line. This is probably a consequence of the fact that the straight horizontal offset L is usually known, whereas the length of the beam or cable in its deformed configuration is of secondary importance.

In order to build the following development on these commonly adopted formulations, we abandon next the representation of the governing equations with a Lagrangian coordinate s and the inclination $\theta(s)$. Instead, a Eulerian (or straight) coordinate x is introduced, and the deformed configuration is represented by a distance $y(x)$ referring to a straight line, see Fig. 2. It is clear that such a Eulerian coordinate is well adapted to the problem at hand where the horizontal length L (and not the curvilinear length ℓ) is known.

The first step in a patching asymptotics approach is to recognize the existence of distinct sub-domains with different responses, modeled if possible with well-known simpler theories. In this case, we admit that the general response may be represented by the connection of a catenary in the outer domain $x \in [D; L - D]$ and a (nonlinear) beam in the boundary layers $x \in [0; D]$ and $x \in [L - D; L]$. The inclinations of the catenary and respectively of the beam are developed independently in each part of the domain. They are then patched, i.e. the finite extent of the boundary layer D is adapted in order to restore the continuity of the slope in the deformed configuration.

At this stage, it is worth mentioning that the usual dimensionless parameters given in (4) are hardly exploitable in practice, precisely because ℓ is unknown. As compensation, similar quantities

are introduced

$$\bar{\varepsilon}^2 = \frac{EI}{wL^3} \quad \text{and} \quad \bar{\eta}^2 = \frac{H}{wL}. \quad (5)$$

They are just slightly different in most cases and start differ significantly from ε and η for slack cables. Notice also that the dimensionless extent of the boundary layer $\delta = D/L$ is supposed to be a small parameter in this study, otherwise classical numerical techniques would be applied. The objective of this paper is to provide a reliable estimation of $\delta(\bar{\varepsilon}, \bar{\eta})$.

Catenary Solution in the Outer Domain

Because of symmetry, the catenary solution is studied for $x_c \in [0; \frac{L}{2} - D]$, with $x_c = 0$ corresponding to the horizontal slope abscissa, see Fig. 2-b. The deformed configuration $y_c(x_c)$ takes a well-known expression (Irvine 1975); in a dimensionless formulation, it reads

$$\mathcal{Y}_c = \mathcal{Y}_{c,o} + \bar{\eta}^2 \cosh \left(\frac{\xi_c}{\bar{\eta}^2} \right). \quad (6)$$

where $\xi_c = x_c/L$ and $\mathcal{Y}_c(\xi_c) = y_c(\xi_c L)/L$. The tangent of the cable inclination (i.e. the slope) at the connection with the boundary layer is obtained by setting $\xi_c = \frac{1}{2} - \delta$ in the derivative $\mathcal{Y}'_c(\xi_c)$.

It writes

$$\hat{m}_c = \sinh \left(\frac{\frac{1}{2} - \delta}{\bar{\eta}^2} \right) \quad (7)$$

where the hat denotes a quantity related to the connection abscissa. The axial force $N_c(\xi_c L)$ along the catenary is given as

$$\frac{N_c}{H} = \cosh \left(\frac{\xi_c}{\bar{\eta}^2} \right) \quad (8)$$

but is more conveniently represented by its decomposition with a constant horizontal force H and a vertical component $V(\xi_c L) = H \sinh(\xi_c/\bar{\eta}^2)$. For $\xi_c = \frac{1}{2} - \delta$, the dimensionless forces related to these two components of the internal force are

$$\frac{\hat{V}}{wL} = \bar{\eta}^2 \sinh \left(\frac{\frac{1}{2} - \delta}{\bar{\eta}^2} \right) \quad \text{and} \quad \frac{\hat{H}}{wL} = \bar{\eta}^2, \quad (9)$$

see Fig. 2-b. They are considered as external forces applied at the end of the nonlinear beam in the inner region.

Although one may admit that the catenary solution is obtained by neglecting the bending stiffness of the cable, it is still possible to determine the curvature in the deformed configuration, from geometric relations, and then to establish a bending moment profile $M_c(\xi_c L)$ along the catenary. With the dimensionless numbers, it is given by

$$\frac{M_c}{EI/L} = \frac{1}{\bar{\eta}^2} \operatorname{sech}^2 \left(\frac{\xi_c}{\bar{\eta}^2} \right). \quad (10)$$

In particular, at the end of the catenary domain, for $\xi_c = \frac{1}{2} - \delta$, the bending moment is symbolized by \hat{M} , see Fig. 2-b. This bending moment is also applied at the tip of the nonlinear beam. As will become clearer later, this actually aims at restoring the continuity between the catenary and beam solutions up to the second order, instead of just the first one if a standard patching method was used. This naturally provides a more accurate response.

Beam Solution in the Inner Domain

The nonlinear beam in the boundary layer is depicted in Fig. 2-c. From standard nonlinear beam theory, its deflection $y_b(x_b)$ is governed by the second order differential equation

$$EI y_b'' = \frac{1}{2} w(D - x_b)^2 + \hat{V}(D - x_b) - \hat{M} - \hat{H}(y_b(D) - y_b) \quad (11)$$

with the boundary conditions $y_b(0) = 0$ and $y_b'(0) = 0$. Equation (11) accounts for the large displacements of the beam, as indicated by the last term, whilst local rotations are assumed to be small, as indicated in the left-hand side by the replacement of the actual curvature by the second derivative of a transverse displacement. This assumption prevents the beam to shorten or extent horizontally in its deformed configuration. In a dimensionless formalism and considering (9)-(10), this governing equation is also written

$$\bar{\varepsilon}^2 \mathcal{Y}_b'' = \frac{1}{2} (\delta - \xi_b)^2 + \bar{\eta}^2 (\delta - \xi_b) \sinh \left(\frac{\frac{1}{2} - \delta}{\bar{\eta}^2} \right) - \frac{1}{\bar{\eta}^2} \operatorname{sech}^2 \left(\frac{\frac{1}{2} - \delta}{\bar{\eta}^2} \right) - \bar{\eta}^2 (\mathcal{Y}_b(\delta) - \mathcal{Y}_b) \quad (12)$$

where $\xi_b = x_b/L$ and $\mathcal{Y}_b(\xi_b) = y_b(\xi_b L)/L$. After some calculus and simplifications, this equation is solved and the slope at the connection with the catenary solution is expressed as

$$\hat{m}_b = \frac{\bar{\varepsilon}}{\bar{\eta}^3} \tanh \left(\frac{\bar{\eta}}{\bar{\varepsilon}} \delta \right) \tanh^2 \left(\frac{\frac{1}{2} - \delta}{\bar{\eta}^2} \right) - \frac{\delta}{\bar{\eta}^2} \operatorname{sech} \left(\frac{\bar{\eta}}{\bar{\varepsilon}} \delta \right) + \sinh \left(\frac{\frac{1}{2} - \delta}{\bar{\eta}^2} \right) \left[1 - \operatorname{sech} \left(\frac{\bar{\eta}}{\bar{\varepsilon}} \delta \right) \right]. \quad (13)$$

Fig. 3: Patching asymptotics solutions for $\bar{\varepsilon} = 0.05$ and $\bar{\eta} = 1$ resulting from a nonlinear (a,c) or linear (b,d) beam model, and considering (a,b) or not (c,d) the reconnection of the bending moment \hat{M} .

Equating now \hat{m}_c and \hat{m}_b from (7) and (13) provides an equation in δ

$$\frac{\delta}{\bar{\eta}^2} + \sinh\left(\frac{\frac{1}{2} - \delta}{\bar{\eta}^2}\right) = \frac{\bar{\varepsilon}}{\bar{\eta}^3} \sinh\left(\frac{\bar{\eta}\delta}{\bar{\varepsilon}}\right) \tanh^2\left(\frac{\frac{1}{2} - \delta}{\bar{\eta}^2}\right) \quad (14)$$

that needs to be solved in order to determine the extent of the boundary layer $\delta(\bar{\varepsilon}, \bar{\eta})$.

The patchability of inner and outer solutions may be discussed by analyzing the existence and uniqueness of solutions to (14). A comprehensive study of this matter goes beyond the scope of this paper. However, it is interesting to notice that the left hand side of (14) is strictly positive for $\delta = 0$ while the right hand side is equal to zero. Moreover, the asymptotic behaviour of (14) for $\delta \rightarrow +\infty$ yields $\exp(\delta/\bar{\eta}^2)/2$ to the left against $\bar{\varepsilon} \exp(\bar{\eta}\delta/\bar{\varepsilon})/2\bar{\eta}^3$ to the right. Expecting $1/\bar{\eta}^2$ to be smaller than $\bar{\eta}/\bar{\varepsilon}$ in interesting cases, the right hand side eventually becomes larger than the left one. As both sides are continuous functions of δ , this indicates the existence of at least one solution; in other words patchability.

Once the extent of the boundary layer $\delta(\bar{\varepsilon}, \bar{\eta})$ is determined, a back-substitution in the respective solutions valid in the catenary domain y_c and in the beam domain y_b provides the deformed configuration of the cable.

As an example, Fig. 3-a represents the cable inclination, i.e. $\arctan \mathcal{Y}'$, for $\bar{\varepsilon} = 0.05$ and $\bar{\eta} = 1$. The exact solution of (14) provides $\delta = 0.3254$ which is considered as a reference solution. The patched solutions (solid line) virtually coincide with the reference result (dotted line), obtained with a full numerical solution of (2)-(3) with the boundary condition $\theta_0 = \theta_\ell = 0$. Details are given next about the computation of this reference solution. The sketches to the left illustrate the reference deformation, axial force and bending moment.

Other Beam Models in the Inner Domain

The nonlinear beam with large displacements and small rotations, as considered before, is an intermediate model between a full nonlinear beam (heavy elastica) and a linear beam with small displacements.

On one hand, a fully nonlinear beam model with large rotations is too complex to solve this problem with a straight Eulerian formulation (Denoël and Detournay 2011). Furthermore, the only known analytical solution is obtained for the weightless elastica; it involves elliptic functions which are not convenient to work within this context.

On the other hand, a linear beam model is probably too approximate in case the beam has to be connected to a cable with a realistic sag. However, if such a model was considered, dropping thus the last term in (12), the slope at the connection point would be given as

$$\hat{m}_{b,lin} = -\frac{\delta}{\bar{\eta}^2} \operatorname{sech}^2\left(\frac{\frac{1}{2} - \delta}{\bar{\eta}^2}\right) + \frac{\delta^2}{6\bar{\varepsilon}^2} \left(\delta + 3\bar{\eta}^2 \sinh\left(\frac{\frac{1}{2} - \delta}{\bar{\eta}^2}\right)\right) \quad (15)$$

instead of (13).

Notice there are few benefits to consider this linear model as it results in analytical expressions that are as complex as in the former case, and anyway in a transcendental equation too for δ .

For all these reasons, the nonlinear beam model with large displacements but small rotations seems to be the perfect tradeoff between accuracy and complexity.

As an illustration, the solutions obtained with the linear beam model are represented in Fig. 3-b, for $\bar{\varepsilon} = 0.05$ and $\bar{\eta} = 1$. In that case the cable sag is not negligible (about 1/10th of the span) and the limitations of the small displacement assumption are evident. The extent of the boundary layer is significantly underestimated ($\delta = 0.0735$, instead of $\delta = 0.3254$).

Two supplementary results are also provided in Fig. 3-c and Fig 3-d for the nonlinear and linear beam models, but without reconnecting the bending moment \hat{M} from the catenary domain to the beam one. In that case, the composite solution $\langle \mathcal{Y}_c, \mathcal{Y}_b \rangle$ is not twice differentiable at the connection point. This is clearly identifiable for the nonlinear beam solution (c). The extent of the boundary layer is substantially different from the model including the bending moment in the

catenary solution, i.e. $\delta = 0.1506$ for 3-c, and $\delta = 0.0690$ for 3-d.

It is now obvious that connecting the bending moment is an inexpensive way to provide a more accurate response.

Approximate Expression of the Boundary Layer

The only hiccup in the patching asymptotics solution, that would prevent its simple application, is the need to numerically solve the transcendental equation (14). In fact, an interesting sequence of approximations of the solution δ may be obtained recursively by rewriting (14) as

$$\sinh\left(\frac{\bar{\eta}}{\bar{\varepsilon}}\delta^{(k+1)}\right) = \frac{\bar{\eta}^3}{\bar{\varepsilon}} \frac{\frac{\delta^{(k)}}{\bar{\eta}^2} + \sinh\left(\frac{\frac{1}{2}-\delta^{(k)}}{\bar{\eta}^2}\right)}{\tanh^2\left(\frac{\frac{1}{2}-\delta^{(k)}}{\bar{\eta}^2}\right)} \quad (16)$$

i.e. collecting in the left hand side the most important nonlinear term (because involving both the $\bar{\varepsilon}$ - and $\bar{\eta}$ -dependencies), and the remaining ones in the right hand side. This formulation is suitable to construct a sequence of approximations that is uniformly convergent for any $\bar{\eta}$. In this expression, the iterate $\delta^{(k+1)}$ for $k \geq 1$ is thus simply obtained from the previous one $\delta^{(k)}$. This sequence is initialized by assuming that the arguments of the hyperbolic functions in the right hand side are very small, which is acceptable for typical operating ranges of $\bar{\eta}$. The first iterate $\delta^{(0)}$ is thus assumed to satisfy

$$\sinh\left(\frac{\bar{\eta}}{\bar{\varepsilon}}\delta^{(0)}\right) = \frac{\bar{\eta}^5}{2\bar{\varepsilon}\left(\frac{1}{2}-\delta^{(0)}\right)^2}. \quad (17)$$

Further assuming that the boundary layer is short, i.e. $\delta^{(0)} \ll 1$, yields

$$\delta^{(0)} = \frac{\bar{\varepsilon}}{\bar{\eta}} \operatorname{arcsinh}\left(\frac{2\bar{\eta}^5}{\bar{\varepsilon}}\right). \quad (18)$$

The successive application of (16) provides a converging series of approximations to the extent of the boundary layer satisfying (14). It is interesting to notice that the construction of that sequence does not require any assumption on the smallness of $\bar{\varepsilon}$; for moderate to large values of the dimensionless rigidity, the sequence still converges, slowlier however.

Fig. 4: Comparison of the exact extent of the boundary layer with approximate solutions.

Fig. 4 represents the solution δ of (14) as well as the first two iterates of this sequence of approximations. The solution is provided for a set of discrete values of $\bar{\varepsilon}$ in 4-a, while a level set representation of δ , $\delta^{(0)}$ and $\delta^{(1)}$ is provided in 4-b. It indicates that the first iterate $\delta^{(0)}$, represented by dash-dot lines, as given by (18) provides a good approximation of the boundary layer for usual applications where the dimensionless bending stiffness is very small. The second iterate $\delta^{(1)}$ is very close to the exact solution in operating ranges of $\bar{\varepsilon}$ and $\bar{\eta}$.

The shadowed zone corresponds to a part of the parametric space $(\bar{\varepsilon}, \bar{\eta})$ where the exact solution provides a boundary layer larger than 0.5. In that zone, the application of the present patching asymptotic solution fails, in principle, because both boundary layer touch. Actually the method could be amended by omitting the central catenary solution and providing therefore a connection of two nonlinear beams. The resulting solution is as good as the deflections in the beam are small, because the small rotation hypothesis still prevails. In short, it is interesting to notice that the domain of application of the proposed method is rather wide, and most importantly, complements perfectly the zone where a standard numerical simulation may be performed fruitfully.

Validation and Illustrations

In this section, the results obtained with the proposed patching approach –based on the nonlinear beam model and the reconnection of the bending moment– are compared with those of a matching asymptotics approach as well as reference results obtained by numerical integration of the governing differential equation. The difficulty in applying these latter two methods is that the curvilinear length ℓ of the cable is a priori unknown.

In a matching asymptotics approach, the solution of (3) for $s \in [0; \ell]$ with the boundary conditions $\theta_0 = \theta_\ell = 0$ is (Denoël and Detournay 2010)

Fig. 5: Level curves of the relative difference between the Eulerian and Lagrangian lengths $\frac{\ell-L}{L}$, obtained from numerical simulations.

$$\theta(s; \ell) = \arctan \frac{\frac{s}{\ell} - \frac{1}{2}}{\eta^2} - 4 \arctan \left[\tau \exp \left(-\frac{\phi s}{\varepsilon \ell} \right) \right] + 4 \arctan \left[\tau \exp \left(-\frac{\phi \ell - s}{\varepsilon \ell} \right) \right] \quad (19)$$

where $\tau = \tan \left[\frac{1}{4} \arctan \left(\frac{1}{2\eta^2} \right) \right]$ and $\phi = (\frac{1}{4} + \eta^4)^{1/4}$. Substitution of this solution into (2) provides an equation in ℓ that requires to be numerically solved. The distance L between the supports is usually a good initial iterate for that numerical solution. Indeed, for applications where $\bar{\varepsilon} \gg 1$ or $\bar{\eta} \gg 1$, the length of the cable ℓ is very similar to L . The relative difference $(\ell - L)/L$ is represented in Fig. 5. In the range of interest, i.e. out of the grayed zone, the length of the cable is almost not affected by the bending stiffness $\bar{\varepsilon}$. It is clear that, in the presence of very short boundary layers, the length of the cable is essentially dominated by the catenary domain. The insensitivity to $\bar{\varepsilon}$ that is revealed in Fig. 5 indicates that this statement is also valid for a moderate to significant extent of the boundary layer. From (6), the length ℓ_c of the cable in the catenary domain is expressed as

$$\frac{\ell_c}{L} = 2 \int_0^{\frac{1}{2}-\delta} \sqrt{1 + \mathcal{Y}_c'^2} d\xi_c = 2\bar{\eta}^2 \sinh \left(\frac{\frac{1}{2}-\delta}{\bar{\eta}^2} \right) = 1 - 2\delta + \frac{(1-2\delta)^3}{24\bar{\eta}^4} + \mathcal{O} \left(\frac{1}{\bar{\eta}^8} \right). \quad (20)$$

In the regions of the parametric space $(\bar{\varepsilon}, \bar{\eta})$ where the boundary layer is very short, i.e. $\delta \ll 1$, the total length of the cable is similar to ℓ_c , and

$$\frac{\ell - L}{L} \simeq \frac{1}{24\bar{\eta}^4}, \quad (21)$$

which actually corresponds to the vertical asymptotes in Fig. 5.

The numerical solution of the heavy elastica problem is undertaken with a shooting method, as follows. Together with the boundary condition $\theta(0) = \theta_0$, initial guesses for $\theta'(0)$ and ℓ allow the transformation of the boundary value problem (3) to an initial value one. This initial value problem is solved by integration with respect to s along $[0; \ell]$, with an RK4 method. The method is further implemented with an adaptive step procedure in order to accommodate for the short boundary layers. Then the two initial guesses are tuned in order to satisfy the second boundary

Fig. 6: Comparison of patching asymptotics, matching asymptotics and exact numerical solutions.

Illustrations cover various values of $\bar{\eta}$ and $\bar{\varepsilon}$ spanning different orders of magnitude. Only close-up view are provided in order to show the perfect agreement.

condition $\theta(\ell) = \theta_\ell$ as well as the constraint (2) related to the distance between the supports. This set of two nonlinear equations with two unknowns is efficiently solved with a Newton-Raphson procedure. We have to admit however that, for cables with a small bending stiffness $\bar{\varepsilon}$ or for slack cables, the convergence is rather poor in the event that the initial guess is relatively far from the expected solution. Furthermore, in that case, multiple stable solutions to the nonlinear differential equation coexist. They correspond to the addition of curls in the deformed cable, as was already noticed by Euler (Euler 1744). In extreme cases, the basin of attraction of the expected solution (the one without curls) collapses. This difficulty is overcome by considering as initial guesses the results of the matching asymptotics. In the examples below, the tolerances on the convergence criteria are set to strict values in such a way that these numerical results may be considered as the reference solution.

Figure 6 shows the cable inclination obtained with the patching asymptotics approach, the matching asymptotics approach and the exact numerical solution. It is estimated by $\arctan[y'(x)]$ for the first approach, and by $\theta[s(x)]$ for the last two ones. Various solutions are presented that cover several orders of magnitude of the dimensionless parameters $\bar{\varepsilon}$ and $\bar{\eta}$. The results obtained with the three methods show a remarkable agreement.

Moreover, the x-axes of plots (d,e,f), corresponding to a cable with a significant tension, indicate that very short boundary layers are captured properly. In those plots, the matching and patching asymptotics approaches provide very good estimates of the exact solution.

As indicated by the level curves in Fig. 4, the extent of the boundary layer is similar for plots (b) and (d), and similarly for plots (c) and (e). In the case of slack cables ($\bar{\eta} = 1$), where the maximum inclination of the cable reaches approximately 0.5 radians, the patching and matching asymptotics solutions still provide accurate results.

The only disputable case corresponds to plot (a), corresponding to a slack cable but with a large bending stiffness. Actually, it is not expected that the patching asymptotic solution be efficient in that case because the two boundary layers related to each cable end conflict ($\delta > 0.5$ as indicated by the grayed zone). In such a case, the patching asymptotics approach provides no catenary solution and a discontinuous inclination at midspan. However, it is interesting to notice that the crossing of this theoretical limit of applicability comes with a gentle decrease of the performance of the patching asymptotics approach. In practice, the discontinuity may even be computed beforehand, with the method presented in this document, and as long as it remains small compared to the maximum cable inclination, the patching asymptotic solution could be considered.

In this limit case where the structural member behaves as much as a beam as a catenary, the matching asymptotics method is also defeated. Indeed, it slightly overestimates the rotations and sag ($y/L = 0.0792$), while the patching asymptotics method underestimates them ($y/L = 0.0752$). These numbers should be compared to the reference result ($y/L = 0.7670$).

Conclusions

In this paper, we have highlighted some benefits of the patching asymptotics approach in the determination of the deformed configuration of a cable with a small bending stiffness. A specificity of the considered problem is that the length of the cable is assumed to be unknown, while the horizontal distance between the supports is known. This naturally promotes the use of a Eulerian coordinate, for which the patching asymptotics is particular well suited.

Several beam models in the inner regions have been discussed and it turns out that the nonlinear beam model with small rotations and large displacements is a perfect tradeoff between accuracy and simplicity. Globally, the accuracy provided by that model is similar to that obtained with the matching asymptotics approach. A basic difference between patching and matching approaches is that the former one provides a boundary layer with a finite extent, while the latter one does not. This issue may be decisive in case such an information is required.

Also, in order to restore a higher-order compatibility between the inner and outer solutions, a bending moment profile is introduced along the catenary solution. This allows the perfect reconnection of the second derivative of the transverse displacement. This feature goes beyond the customary assets of the patching asymptotics approach, for which a formal application would have allowed the reconnection of the first derivative only. The concept developed here may be generalized by observing that this advanced patching solution is obtained by allocating to the catenary solution a feature of the beam solution, namely the *a posteriori* established bending moment, and similarly by encapsulating in the beam solution a feature of the cable solution, namely the large displacement and the restoring moment generated by the axial force H . We believe this concept could be generalized to other applications.

Another important contribution of the paper is the establishment of approximate solutions for the extent of the boundary layer δ , which makes its application possible without having to solve a transcendental equation.

For these reasons, the patching asymptotics approach appears as a smart way to bridge the gap between difficult perturbation solutions and simple engineering thinking.

Acknowledgments

The idea of considering a patching asymptotics approach for the solution of that problem emerged during a stay of VD at the CSIRO (Commonwealth Scientific and Industrial Research Organization, Perth, Australia), thanks to interesting discussions and interactions with Prof. E. Detournay.

References

- Antman, S. S. (1995). *Nonlinear problems in Elasticity*. Applied Mathematical Sciences. Springer Verlag, Berlin.
- Bieniasz, L. K. (2008). “Adaptive solution of bvp's in singularly perturbed second-order odes,

by the extended numerov method combined with an iterative local grid h-refinement." *Applied Mathematics and Computation*, 198(2), 665–682 Bieniasz, L. K.

Burgess, J. J. (1993). "Bending stiffness in a simulation of undersea cable deployment." *International Journal of Offshore and Polar Engineering*, 3(3), 197–204.

Cluni, F., Gusella, V., and Ubertini, F. (2007). "A parametric investigation of wind-induced cable fatigue." *Engineering Structures*, 29(11), 3094–3105.

Denoël, V. and Detournay, E. (2010). "Multiple scales solution for a beam with a small bending stiffness." *Journal of Engineering Mechanics*, 136(1), 69–77.

Denoël, V. and Detournay, E. (2011). "Eulerian formulation of constrained elastica." *International Journal Of Solids And Structures*, 48(3-4), 625–636.

Esipova, V. (1975). "The asymptotic behavior of solutions of the general boundary value problem for singularly perturbed systems of ordinary differential equations of conditionally stable type." *Differential Equations*, 11(11), 1457–1465.

Euler, L. (1744). *Methodus inveniendi lineas curvas maximi minimive proprietate gaudentes, sive solutio problematis isoperimetrici lattissimo sensu accepti*.

Hinch, E. J. (1991). *Perturbation Methods*, Vol. 1. Cambridge University Press, Cambridge.

Hong, K. J., Kiureghian, A. D., and Sackman, J. L. (2005). "Bending behavior of helically wrapped cables." *Journal of Engineering Mechanics*, 131(5), 500–511.

Irvine, H. M. (1975). "Statics of suspended cables." *Journal of the Engineering Mechanics Division-Asce*, 101(3), 187–205.

Jain, M. K., Iyengar, S. R. K., and Subramanyam, G. S. (1984). "Variable mesh methods for the numerical-solution of 2-point singular perturbation problems." *Computer Methods in Applied Mechanics and Engineering*, 42(3), 273–286.

Kevorkian, J. and Cole, J. D. (1996). *Multiple Scale and Singular Perturbation Methods*. Applied Mathematical Sciences. Springer Verlag, Berlin.

Kumar, M., Kumar Mishra, H., and Singh, P. (2009). "A boundary value approach for a class of linear singularly perturbed boundary value problems." *Advances in Engineering Software*, 40(4), 298–304.

Levien, R. (2008). "The elastica: a mathematical history." Ph.D. thesis, Ph.D. thesis.

Nayfeh, A. H. (1973). *Perturbation Methods*. Wiley Classics Library. Wiley.

Papailiou, K. O. (1997). "On the bending stiffness of transmission line conductors." *IEEE Transactions on Power Delivery*, 12(4), 1576–1583.

Quarteroni, A. and Valli, A. (1994). *Numerical approximation of partial differential equations*. Springer Verlag. Springer Verlag.

Rao, S. C. S. and Kumar, M. (2007). "B-spline collocation method for nonlinear singularly-perturbed two-point boundary-value problems." *Journal of Optimization Theory and Applications*, 134(1), 91–105 Rao, S. C. S. Kumar, M.

Reddy, Y. N. and Chakravarthy, P. P. (2004). "Numerical patching method for singularly perturbed two-point boundary value problems using cubic splines." *Applied Mathematics and Computation*, 149(2), 441–468.

Rienstra, S. W. (1987). "Analytical approximations for offshore pipelaying problems." *Proceedings of the International Conference on Industrial and Applied Mathematics*, Paris-la-Villette (June 29–July 3 1987).

Schmeiser, C. and Weiss, R. (1986). "Asymptotic analysis of singular singularly perturbed boundary-value-problems." *Siam Journal on Mathematical Analysis*, 17(3), 560–579.

Stynes, M. and Oriordan, E. (1986). "A finite-element method for a singularly perturbed boundary-value problem." *Numerische Mathematik*, 50(1), 1–15.

Timoshenko, S. P. and Goodier, J. N. (1987). *Theory of Elasticity*. McGraw-Hill Book Company, New-York, third edition edition.

Traeger, W. and Kollegger, J. (2010). "Fatigue testing of stay cables at resonant frequency." *IASMAS 2010, Bridge Maintenance, Safety, Management and Life-Cycle Optimization*, 3589–3592.

Wang, C. Y. (1986). "A critical review of the heavy elastica." *International Journal Of Mechanical Sciences*, 28(8), 549–559.

Wang, W., Kosor, R., and Bai, Y. (2011). "Fatigue analysis on multi-spanning pipelines." *Harbin Gongcheng Daxue Xuebao/Journal of Harbin Engineering University*, 32(5), 560–564.

Wei, X. and Qiang, S. (2011). "Fatigue performance of anchorage zone for long-span single pylon cable-stayed bridge." *Xinan Jiaotong Daxue Xuebao/Journal of Southwest Jiaotong University*, 46(6), 940–945.

Wolfe, P. (1991). "Asymptotic analysis of a rod with small bending stiffness." *Quarterly of Applied Mathematics*, 49(1), 53–65.

Figure 1: (a) the catenary problem where the deflection of a cable under tension H is to be determined and (b) the considered problem which is similar but with imposed end rotations. Notice the cable length ℓ is unknown in both cases.

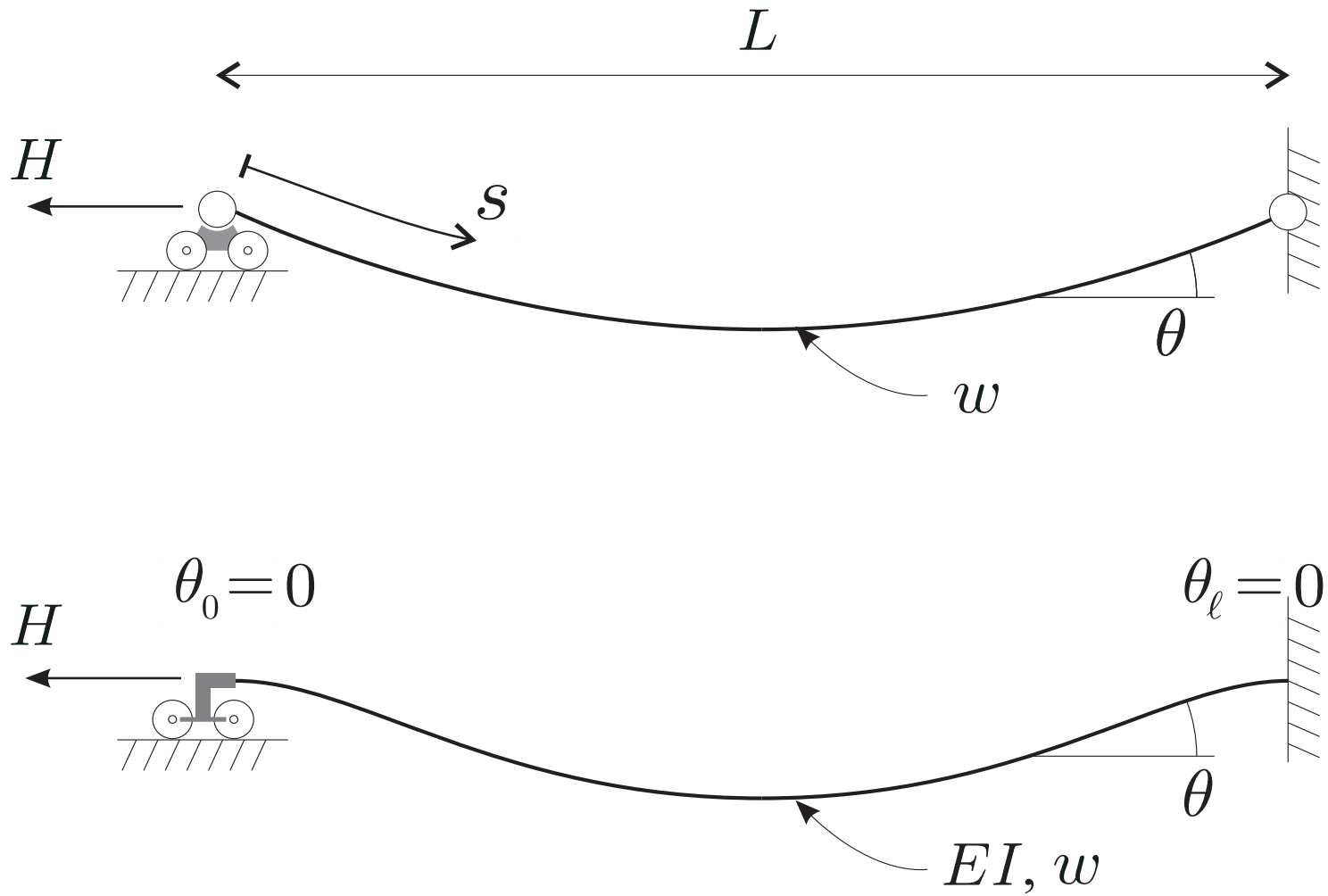
Figure 2: a) Decomposition of the beam into several sub-domains that are patched; (b) catenary solution in the outer domain; (c) beam solution in the inner domain.

Figure 3: Patching asymptotics solutions for $\bar{\varepsilon} = 0.05$ and $\bar{\eta} = 1$ resulting from a nonlinear (a,c) or linear (b,d) beam model, and considering (a,b) or not (c,d) the reconnection of the bending moment \hat{M} .

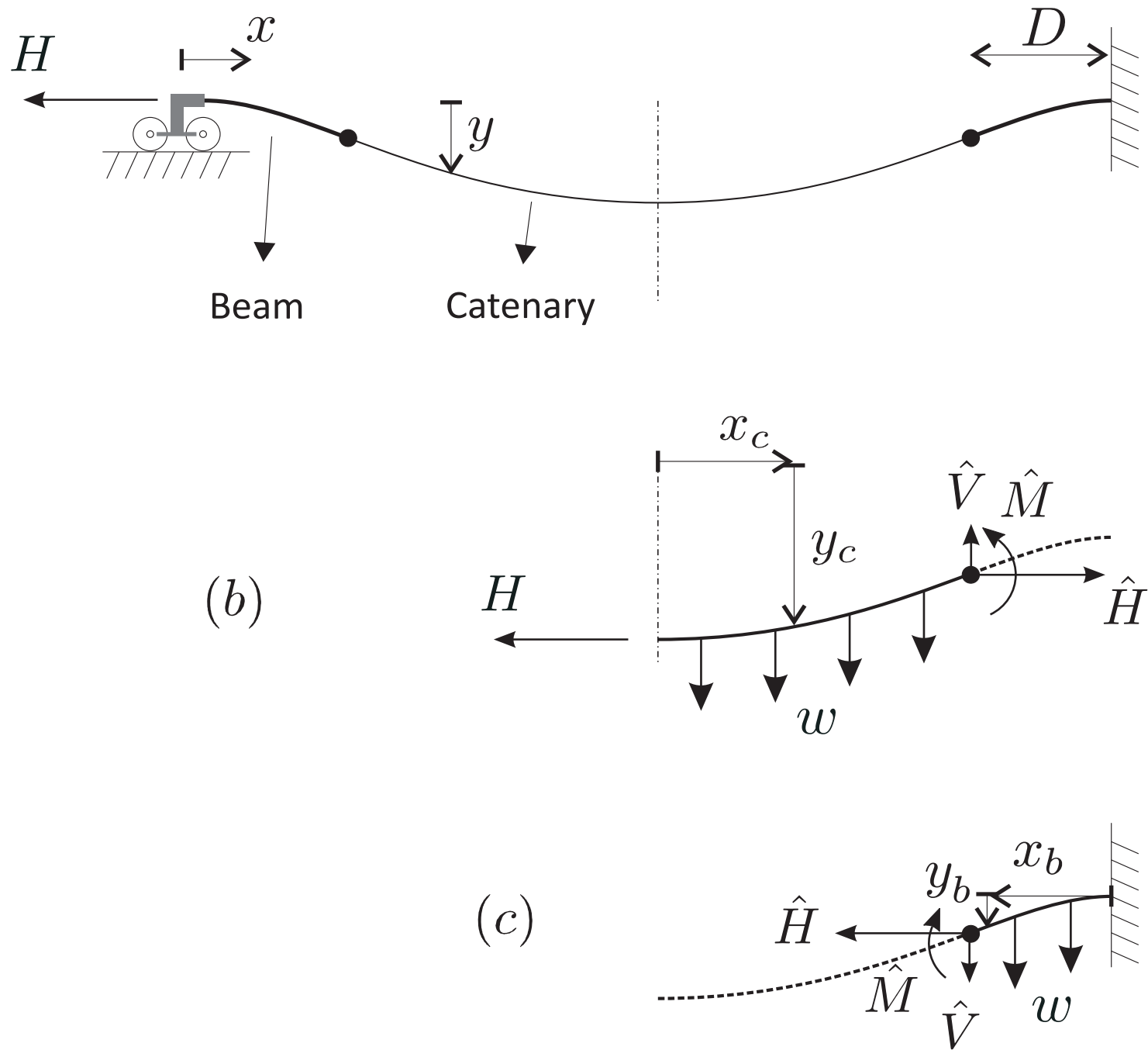
Figure 4: Comparison of the exact extent of the boundary layer with approximate solutions.

Figure 5: Level curves of the relative difference between the Eulerian and Lagrangian lengths $\frac{\ell-L}{L}$, obtained from numerical simulations.

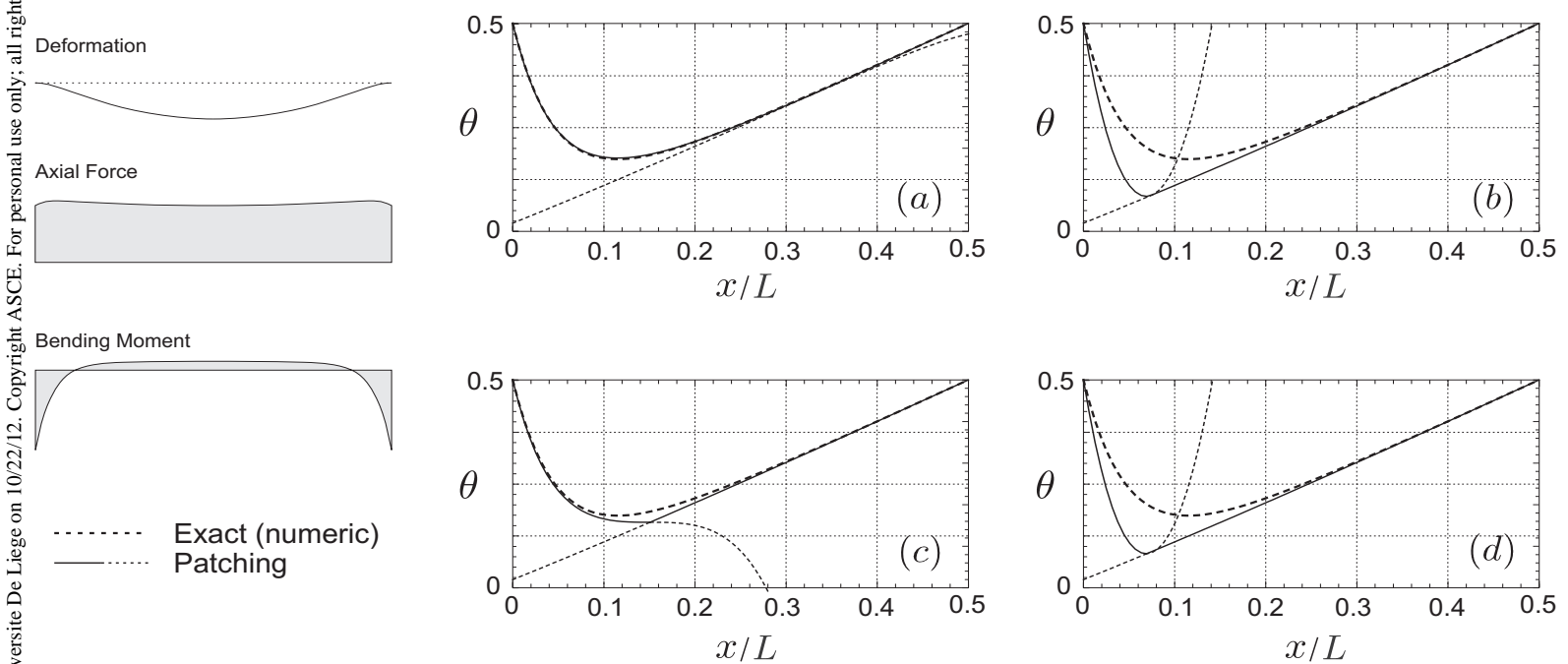
Figure 6: Comparison of patching asymptotics, matching asymptotics and exact numerical solutions. Illustrations cover various values of $\bar{\eta}$ and $\bar{\varepsilon}$ spanning different orders of magnitude. Only close-up view are provided in order to show the perfect agreement.



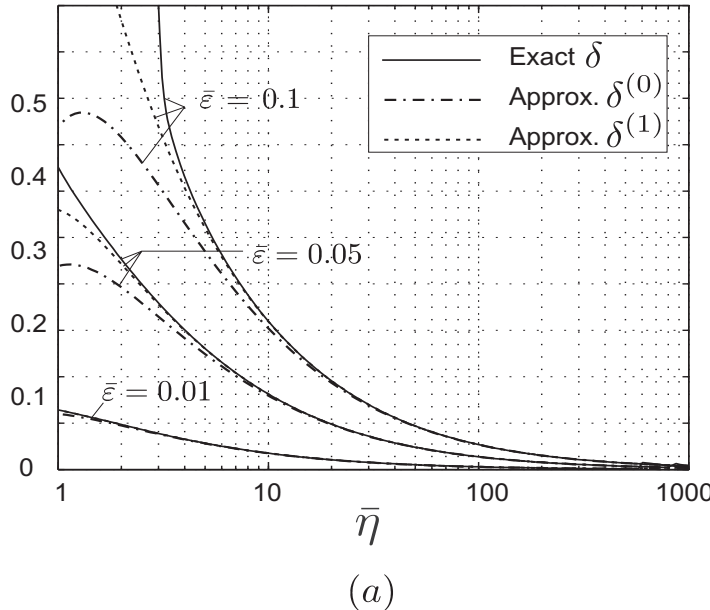
Accepted Manuscript
Not Copyedited



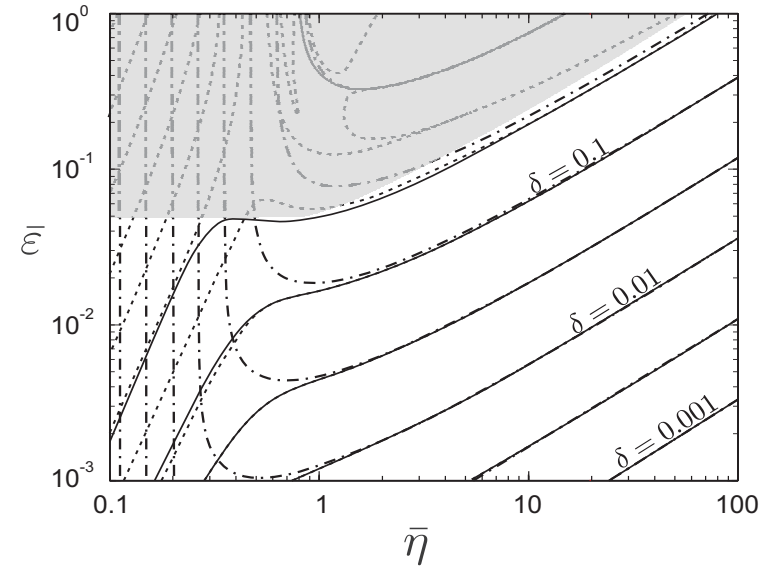
Accepted Manuscript
Not Copyedited



Accepted Manuscript
Not Copyedited

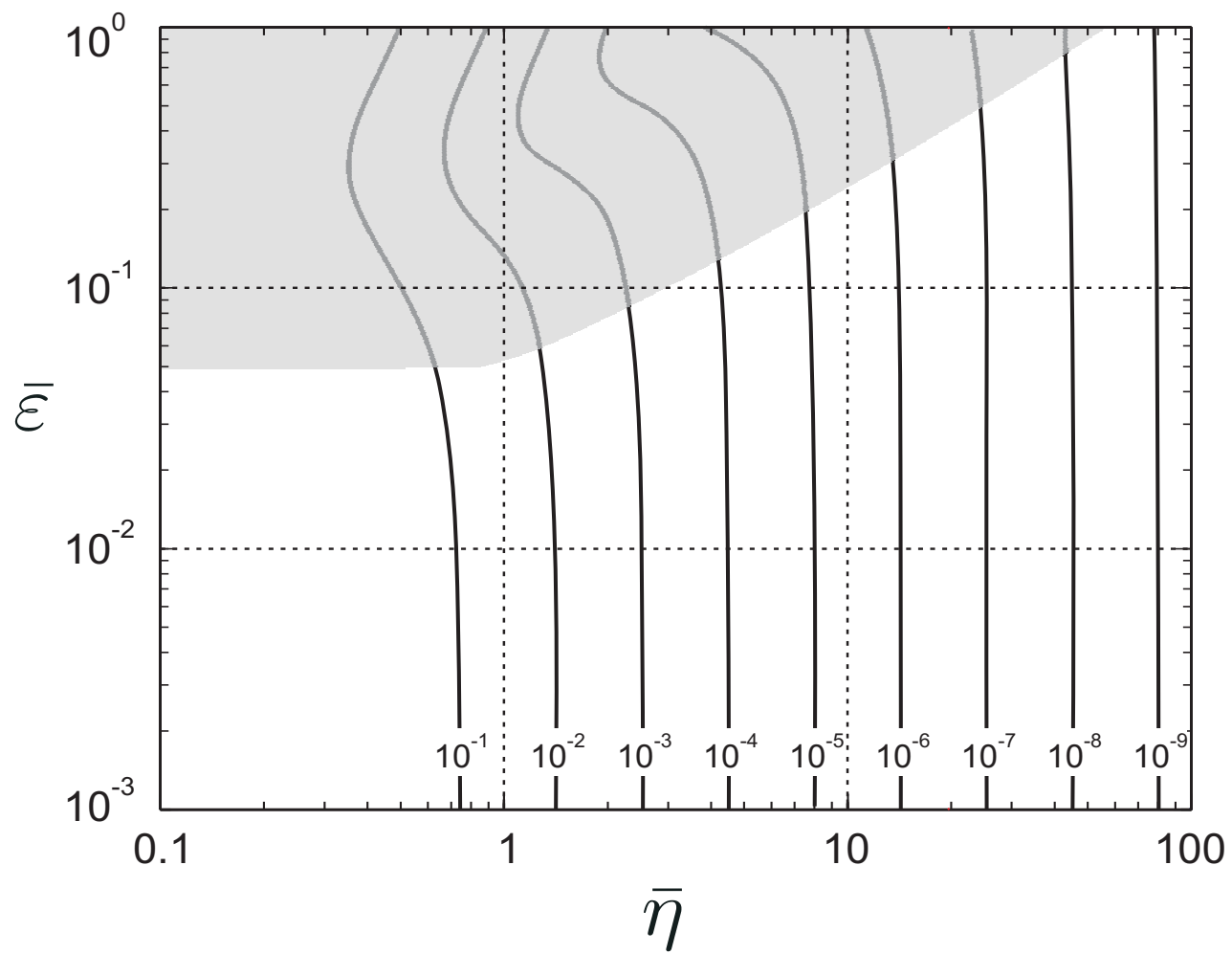


(a)

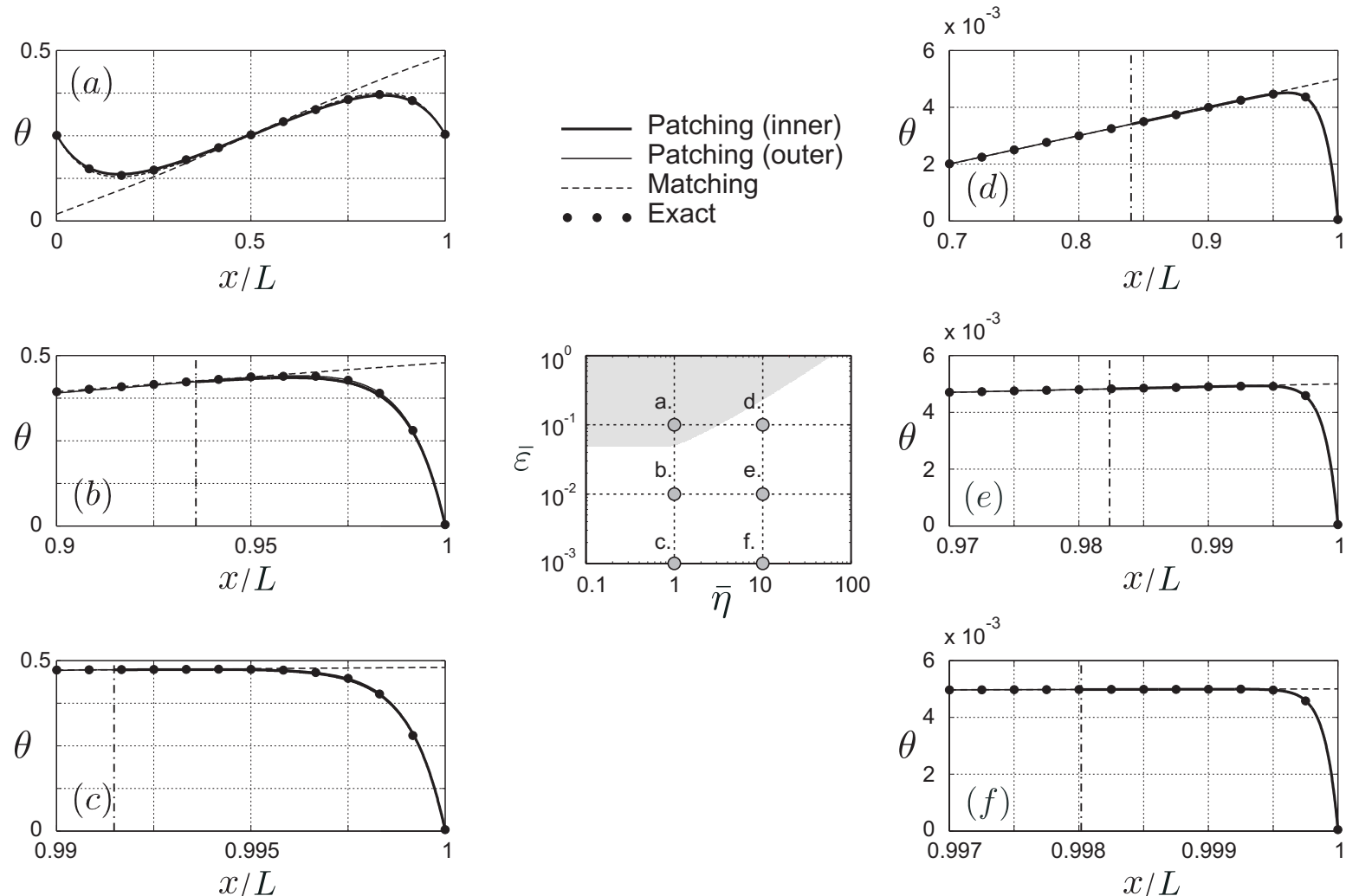


(b)

Accepted Manuscript
Not Copyedited



Accepted Manuscript
Not Copyedited



Accepted Manuscript
Not Copyedited